HYDROLOGIC PROCESSES AT INTERFACES CAUSE CHANGES IN GEOPHYSICAL SIGNATURES: A FIELD STUDY

By

BRADEN HRENCHER

Bachelor of Science in Geology

Fort Hays State University

Hays, Kansas

2015

Submitted to the Faculty of the
GraduateCollege of the
OklahomaStateUniversity
in partial fulfillment of
the requirements for
the Degree of
MASTER OF SCIENCE
May, 2018

HYDROLOGIC PROCESSES AT INTERFACES

CAUSE CHANGES IN GEOPHYSICAL SIGNATURES:

A FIELD STUDY

Thesis Approved:

Javier Vilcaez

Thesis Chair

Estella Atekwana

Thesis Adviser

Ahmed Ismail

ACKNOWLEDGEMENTS

First and foremost, I would like to thank my committee: Dr. Javier Vilcaez (chair), Dr. Estella Atekwana (adviser), and Dr. Ahmed Ismail (member) for their continued technical support throughout my time at Oklahoma State University. I especially acknowledge Dr. Estella Atekwana for her support, funding, and guidance during my studies. I also would like to especially acknowledge Sundeep Sharma for his time, knowledge, and guidance throughout this process. Partial funding for this project was provided by Chevron Energy Technology Company (grant CW852844 to Dr. Estella Atekwana) and use of Oklahoma State University's SEM facility was provided by NSF grant EAR-0722410 (to Dr. Estella Atekwana). Field access to the Bemidji, MN site was provided by the United States Geological Survey. Dr. Priyank Jaiswal, Sundeep Sharma, and Caitlin Redmond helped with fieldwork and data acquisition.

I would like to thank all the administrative bodies and faculties of the Boone Pickens School of Geology (BPSoG). Without their support and encouragement, this thesis would not have been possible. All the support and friendship I received from my friends and colleagues at BPSoG played an astronomical role and helped me through the toughest of times.

Lastly, I would like to thank my parents and friends. Their encouragement and optimism throughout my graduate career has been incredibly beneficial and none of this could have been possible without their support.

Name: BRADEN HRENCHER

Date of Degree: MAY, 2018

Title of Study: HYDROLOGIC PROCESSES AT INTERFACES CAUSE CHANGES IN GEOPHYSICAL SIGNATURES: A FIELD STUDY

Major Field: GEOLOGY

Abstract: Enhanced biogeochemical activity resulting from the mixing of complementary terminal electron acceptors and electron donors characterize many classic transition environments. Few studies have been conducted to better understand the role that water oscillations or groundwater-surface water mixing have on the biogeochemistry and microbial composition. The need for imaging technologies that can identify biogeochemical hot zones in the subsurface and help guide microbial and geochemical sampling so that these zones can be better studied and understood is very important. In this study, the use of surface seismic methods in detecting the end product of biogeochemical processes driven by hydrologic processes is demonstrated using a hydrocarbon contaminated site in Bemidji, Minnesota as an example. The experiment uses the Multichannel Analysis of Surface Wave (MASW) method to analyze shear wave along two profiles. Results show a high shear wave velocity layer (>220 m/s) coincident with the water table oscillation zone. Environmental scanning electron microscope images integrated with core description and analysis, suggest the presence of biofilms may explain the higher shear wave velocity. This finding is consistent with other shear wave experiments, both in the lab and field setting. We confirm that the fluctuating water table drives the biogeochemical processes which in turn drive the geophysical changes recorded. Our results may be applicable to the remote detection of biogeochemical hot zones and can help guide geochemical and microbial sampling in these environments.

TABLE OF CONTENTS

Chapter Page

LIST OF FIGURES

Figure Page

Figure Page

Figure Page

CHAPTER I

INTRODUCTION

Classic environmental transition environments such as hyporheic zones (Figure 1), contaminant fringes, water table fluctuation zones, and freshwater-saltwater interfaces are characterized by enhanced rates of biogeochemical activity resulting from the mixing of complementary terminal electron acceptors and electron donors (Hedin et al., 1998; McClain et al., 2003; Craig et al., 2010; Stegen et al., 2016).

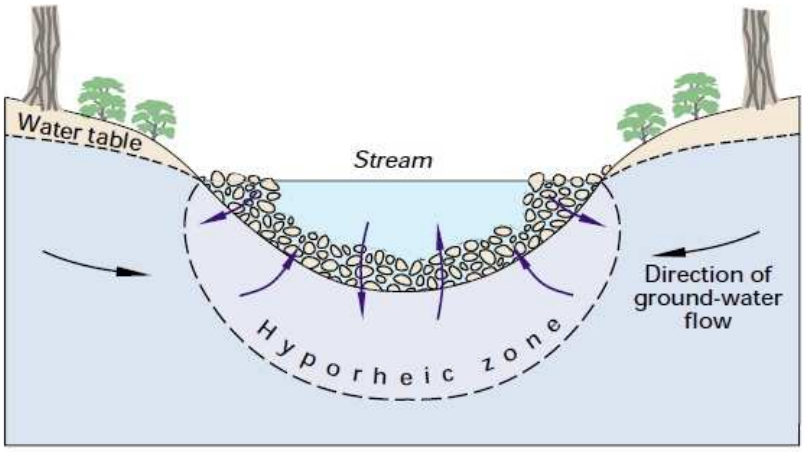

Figure 1 – Image depicting the hyporheic zone as an environmental transition zone. Courtesy of USGS Circular 1139.

The water table transition zone, which separates the soil from the groundwater below, plays a large role in the regulation of the flows of carbon, nutrients, and contaminants at a watershed scale (*Triska et al., 1989; Hefting et al., 2004; Sophocleous, 2002; Hancock et al., 2005)*. Few studies have been conducted to better understand the role that water oscillations or groundwater-surface water mixing have on the biogeochemistry and microbial community composition. In an experimental study by Rezanezhad et al. (2014), the authors documented that transient redox conditions induced by water table oscillations stimulated and enhanced microbial oxidation of soil organic matter, leading to the pronounced depletion of particulate organic carbon (Figure 2) within the transition zone. In contrast, the stable water condition showed minimal changes in redox oscillations and organic carbon oxidation. In the above study, the authors observed no significant differences in the microbial community within the water table fluctuation zone and that of the same depth in the constant water table control treatment. Thus, fluctuations of the water table greatly affect the geochemical and biological functioning of soils (*Rezanezhad et al., 2014*), and may cause large temporal variations in local redox conditions and matrix potential (*Vorenhout et al, 2004; Haberer et al., 2012)*. Changes in the soil matrix can affect diffusion of nutrients and gases (*Griffiths et al., 2005; Schimel et al., 2007; Drenovsky et al., 2004)*, while existing data shows modification of biogeochemical and microbial dynamics in subsurface environments caused by oscillating redox conditions (*Weber et al., 2009; Blodau and Moore, 2003; Pett-Ridge et al., 2006)*. Pett-Ridge and Firestone (2005) note that compared to subsurface communities living in stable conditions, microbial communities in the same depth interval over which the water table fluctuates, can adapt to the continuous changes in

redox potential and water saturation by developing an increased flexibility and functional diversity, thus resulting in enhanced organic carbon turnover (*Stegen et al., 2016*).

Despite the obvious importance of transitional environments in driving key biogeochemical cycles (e.g., carbon cycle), the key drivers (e.g., shifts in microbial communities) of these changes are currently understudied due to the spatial complexity and temporally dynamic nature of these environments (*Stegen et al., 2016*). Current techniques for investigating biogeochemical processes within transitional environments rely heavily on the characterization of spatiotemporal changes in electron donors, terminal electron acceptors, and microbial biomass or activity (*Craig et al., 2010; Stegen et al., 2016*). Nonetheless, these studies may not truly capture the biogeochemical hot zones. There is a need for imaging technologies that can identify biogeochemical hot zones in the subsurface and help guide microbial and geochemical samplings so that these zones can be better studied and understood. Over the last decade, numerous studies have documented the fact that high resolution geophysical techniques can be used to investigate microbial processes within the subsurface (*Atekwana and Slater, 2009 and references there in)* at a high spatial and temporal resolution not achievable by any other techniques (*Heenan et al., 2015)*.

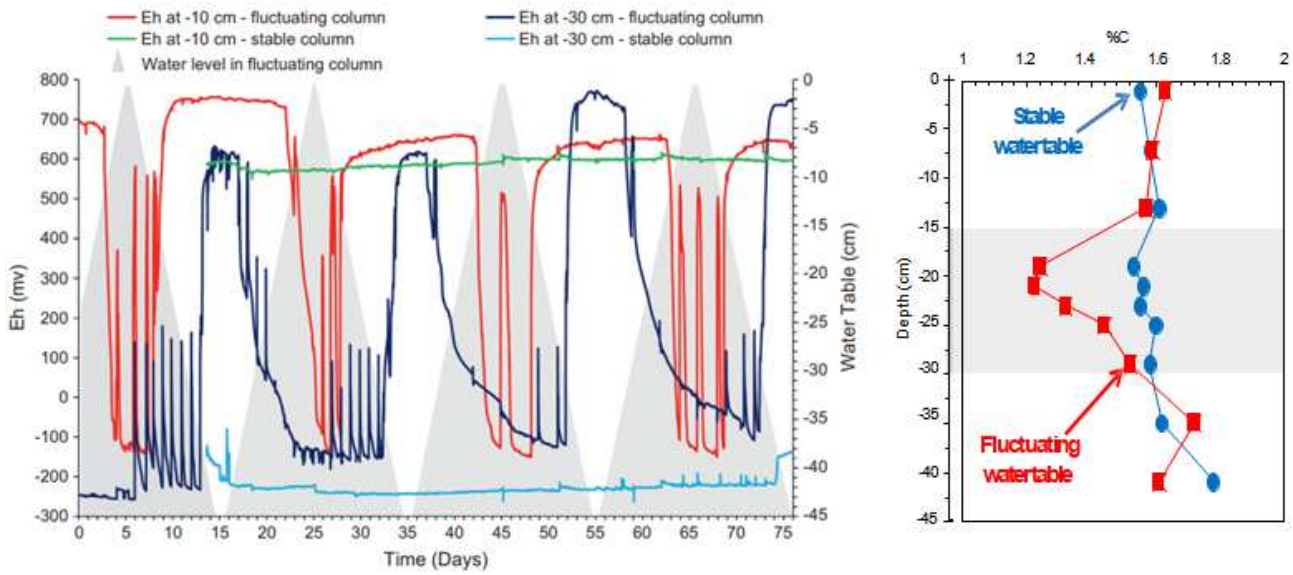

Figure 2. a) – Transient redox conditions induced by fluctuating water table and **b)** change of particulate organic carbon concentration in the fluctuating water table compared to a stable water table. (Figure modified from Rezanezhad et al. 2014).

Numerous examples exist in the geophysical literature linking geophysical property changes to microbial activity. For example, magnetic susceptibility studies at hydrocarbon contaminated sites by Rijal et al. (2010) and Atekwana et al. (2014) documented maximal excursions in the magnetic susceptibility within the water table fluctuation zone and suggested this as the most microbially active zone. In a related study, Beaver et al. (2016) used the magnetic susceptibility data of Atekwana et al. (2014) to guide their microbial sampling and revealed the presence of methanogenic microbial communities within the zone of enhanced magnetic susceptibility. In a more recent study at a landfill site, Sharma (2017) using seismic techniques documented 50-60% increase in shear wave velocity and an increase in P-wave attenuation of 60-80%

within the water table fluctuation zone. Indeed, scanning electron microscope (SEM) analyses of sediments retrieved from cores at the site, confirmed presence of biofilms, which the author used to suggest that biofilms may have been responsible for the enhancement of the shear wave velocity. The Sharma (2017) study confirmed previous seismic laboratory observations (Davis et al., 2009; 2010, Kwon and Ajo Franklin, 2013; Noh et al., 2016) of the effect of biofilms on seismic wave propagation. The Sharma (2017) study also provided field confirmation of acoustic wave variation from biogeochemical processes occurring within the transition zones. Such knowledge, although instrumental in improving our understanding of the spatial and temporal evolution of biogeochemical process within transitional environments, is limited from many transition environments. Hydrocarbon contaminated sites are bioreactors. Biodegradation of the contaminants cause steep spatial and temporal geochemical gradients that have been characterized by other geophysical methods (Atekwana and Atekwana, 2010 and references there in). The ability of these techniques to characterize this results from changes in the physical environment that should manifest in changes of the acoustic wave velocities. Thus, hydrocarbon contaminated sites may represent an ideal laboratory for identifying biogeochemical hot zones by other geophysical methods. This study extends the Sharma (2017) study at a hydrocarbon contaminated site in Bemidji, Minnesota. The specific objectives were to 1) verify that shear wave velocities are enhanced within the water table fluctuation zone due to enhanced microbial activity and 2) determine if there exists any differences in shear wave velocities between contaminated and uncontaminated regions. To achieve the study objectives, two seismic

profiles were acquired transverse to the long axis of the plume to assess how the velocities change with spatial variability in the biogeochemical processes.

CHAPTER II

STUDY SITE

The study site is the National Crude Oil Spill Fate and Natural Attenuation Research Site located near the town of Bemidji, in north central Minnesota, more specifically 47°34'26.64" N and 95°05'25.88" W.

In 1979, a crude oil pipeline burst, resulting in over 1,700,000 liters of oil being dispersed across the area. Even after initial cleanup methods were performed by the pipeline company, including surface-burning, pump-recovery of liquid crude oil, and basic land farming, an estimated 410 cubic meters of crude oil remained unaccounted for, with a majority present floating on the water table approximately 6-10 meters below the land surface (Figure 4) (*Bennett et al., 1993; Eganhouse et al., 1993*). Out of the two main subsurface oil bodies resulting from the spill, one oil body, identified as the "North Pool", has been the most heavily focused on for research. The site is currently managed by the United States Geological Survey (USGS), with investigations of the site beginning in 1983, and still currently acts as a natural laboratory for further investigation of biophysicochemical processes associated with bioremediation of a crude oil spill (*Cozzarelli et al., 2001; Eganhouse et al., 1993; Hult, 1984*).

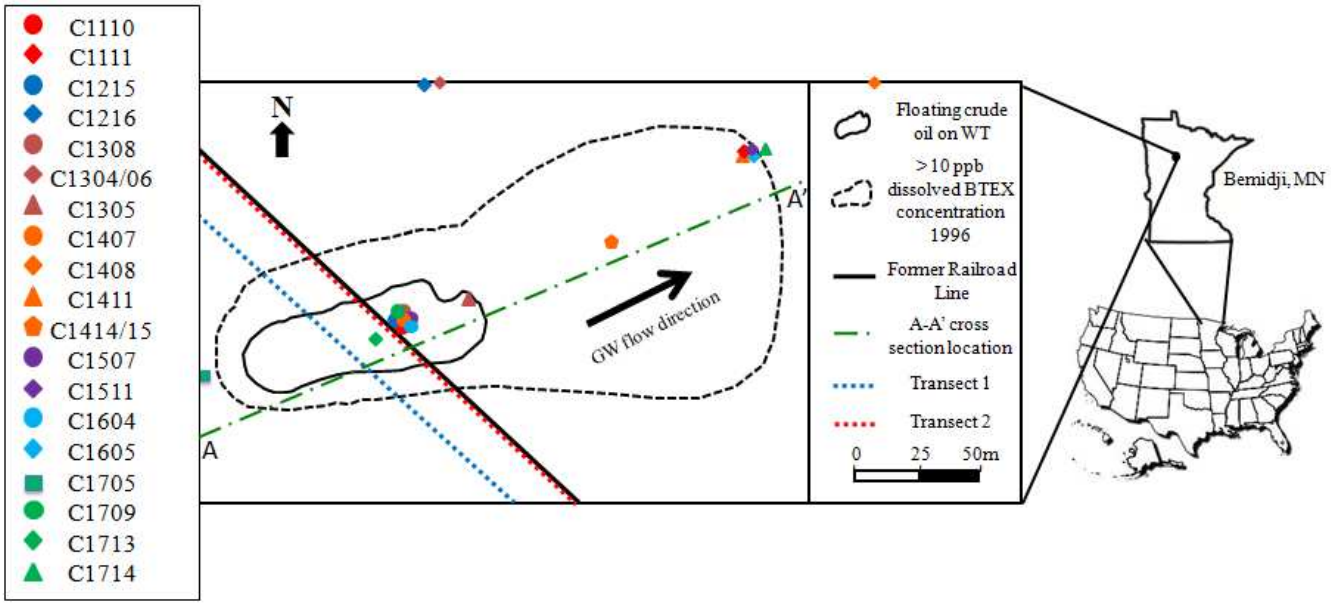

Figure 3 – Bemidji, Minnesota spill site. Blacked dashed polygon shows extent of dissolved crude concentration. Black solid polygon shows floating crude oil on water table. Seismic Transect 1 (T1) and Transect 2 (T2) are shown with blue and red dotted lines respectively. Figure also shows location of cores used for magnetic susceptibility measurements and core analysis since 2011. The first two numbers of each core represent the year retrieved. Figure modified from S. Rossbach (unpublished data).

The geology beneath the main study site consists of approximately 20 meters of moderately calcareous silty sand and outwash glacial deposits, which overlays an unknown thickness of clayey till (*Bennett et al., 1993*). Figure 4 depicts a geologic cross section further explaining layers found within the study area.

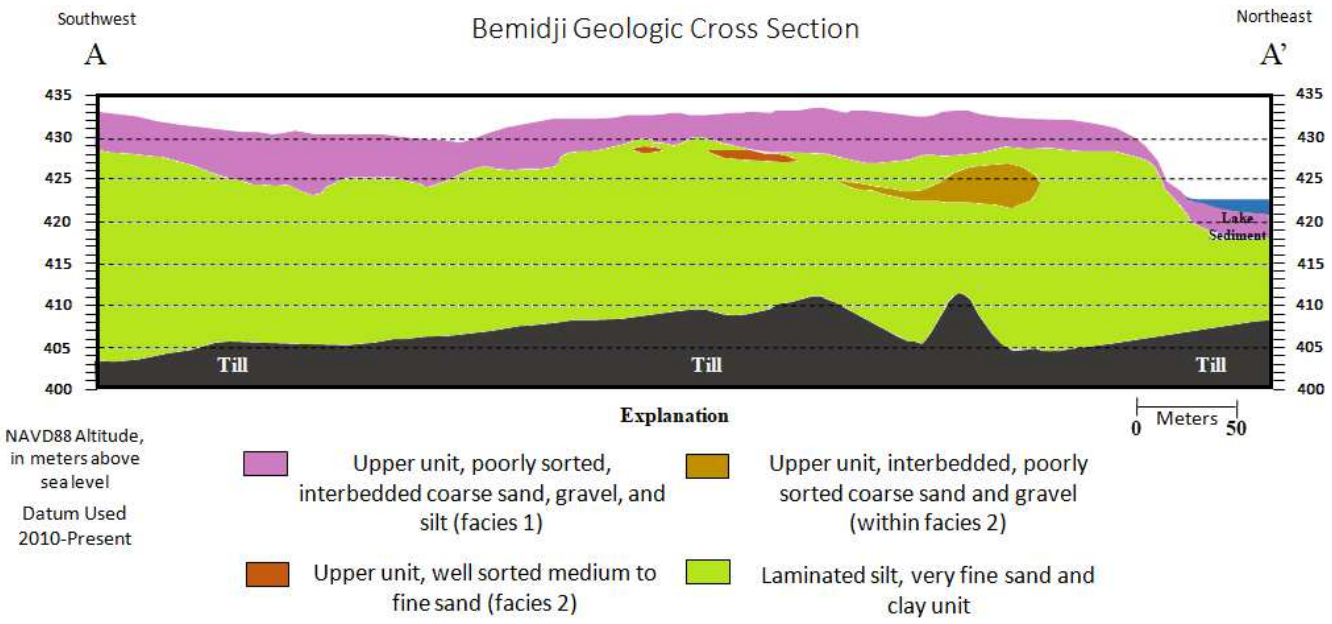

Figure 4 – Geologic cross section of Bemidji spill site study area from SW to NE (refer back to figure 3). Profile extends approximately 100 meters in each direction past dissolved BTEX (benzene, toluene, ethylbenzene, and xylene) concentration portion of the plume from an aerial view. Geology modified from D.A. Franzi (Plattsburgh State University, written commun., 1989 and 1994). Cross section modified from United States Geological Survey Bemidji website (https://mn.water.usgs.gov/projects/bemidji/spatial/Current/xsection.pdf, 5/01/18).

The geologic cross section shows 3 to 6 meters of poorly sorted, interbedded coarse sand, gravel, and silt. The next facies is a well sorted medium to fine sand, with an interbedded, poorly sorted coarse sand and gravel bodies varying from 1 to 5 meters thick in areas. A large laminated silt, very fine sand, and clay unit, approximately 6-7 meters beneath ground level, makes up the majority of the lithology in the area extending from 15-25

meters in thickness beneath the upper units, followed by the lower till layer approximately 25-30 meters beneath ground level.

The climate at the study area includes a mean annual temperature of 3°C (37.4°F) and an annual precipitation rate of approximately 0.58m (*Essaid et al., 2011*). The groundwater flow direction is towards the east-northeast direction and has an average water table fluctuation level of around 1 meter. Seasonal water table fluctuation causes smearing of hydrocarbons with variable thickness of up to 2 meters in the down-gradient portion of the North Pool (*Essaid et al., 2011).* Delin et al. (1998) notes the water table beneath the surface ranges from 0 meters, near an unnamed lake, to a maximum of 11 meters. By averaging values recorded by the USGS from the water observation wells along each transect, the water table is approximately 6 meters deep along transect 1 and approximately 8 meters deep along transect 2. Figure 5 below shows a 10 year fluctuation of water levels at a water observation well located directly between transect 1 and transect 2 within the floating crude oil portion of the plume in which the average water table is around 7 meters deep, as expected.

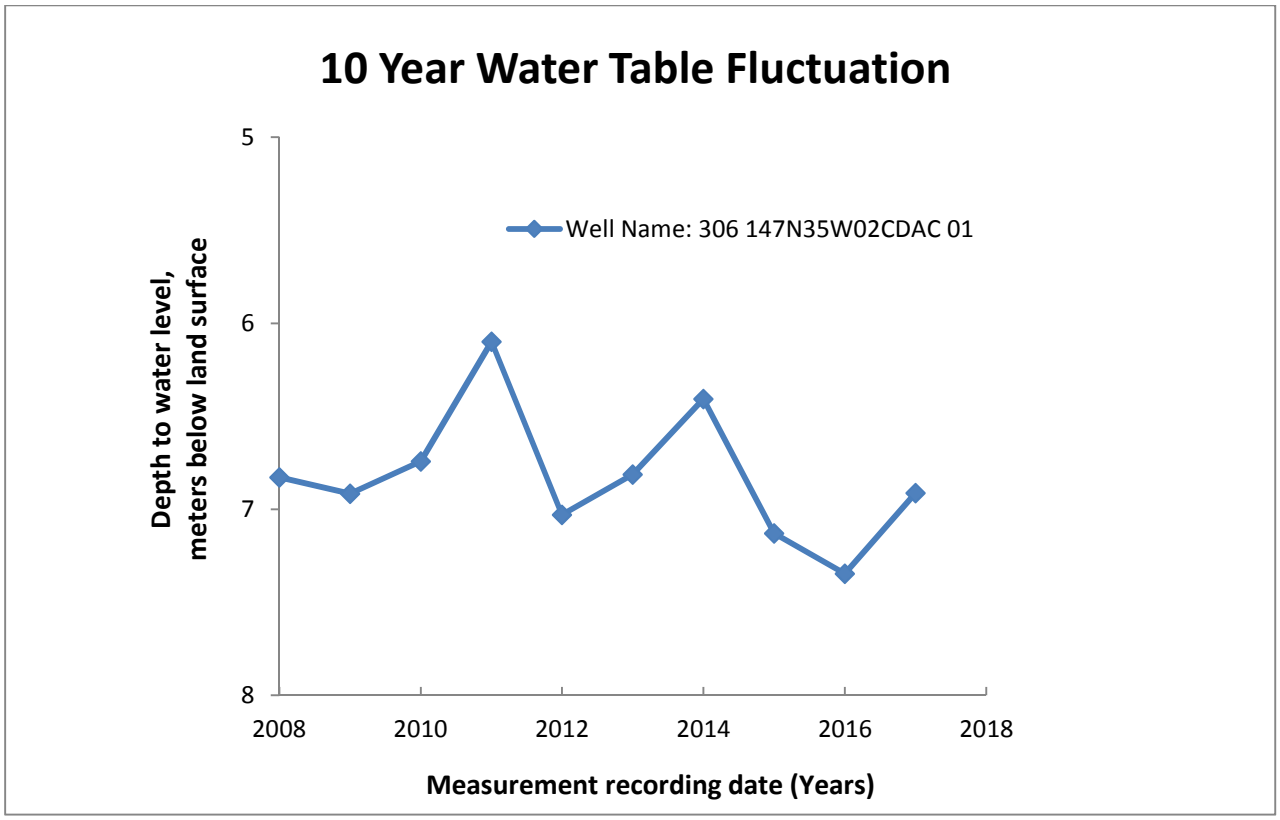

Figure 5 – 10 year water table variation from well name: 306 147N35W02CDAC 01. Well is located directly between transect 1 and transect 2 within the floating crude oil portion of the plume. Data shows a water table fluctuation of approximately one meter, with an average water table of just above 7 meters. Data recorded from USGS website (https://groundwaterwatch.usgs.gov/AWLSites.asp?S=473426095052608&ncd=MBT).

Eight geochemical zones have been identified at the North oil pool, with five being in the saturated zone and three within the unsaturated zone (*Baedecker et al., 1993; Bennett et al., 1993; Delin et al., 1998*). The uncontaminated groundwater is aerobic with dissolved oxygen concentrations between 8 and 9 mg/L, dissolved organic carbon of 2.8 mg/L as C, and low levels of nitrate at 44.8 µg/L as N and sulfate at 2.9 mg/L (*Bennet et*

al., 1993). Within the oil body vicinity, the aquifer is divided into anoxic, transition, and oxic (background) zones. Baedecker at al. (1993) and Lovley et al. (1989) identified that hydrocarbons are predominantly oxidized by methanogenesis and iron reduction, respectively within the anoxic zone. The vadose zone vapor plume near the oil body has low O_2 (< 2%) and high CO_2 (>10%) and CH_4 (>15%) levels (*Atekwana et al., 2014).* The geochemical and microbial studies suggest that iron reduction is an important electron acceptor process occurring within the plume (*e.g., Baedecker et al., 1993*). Dissimulatory iron-reducing bacteria (DIRB) such as *Geobacter bemidjiensis sp* and *Geobacter psychrophilus sp* occur in the contaminated aquifer (*Nevin et al., 2005).* Iron minerals in sediments including geoethite, hematite, magnetite, ferrihydrite, siderite, and maghemite (*Bekins et al., 2001, Atekwana et al., 2014)* have been suggested based off several mineralogical studies within the site as well (*Baedecker et al., 1992, 1993; Tuccillo et al., 1999; Zachara et al., 2004)*.

Several geophysical investigations have been conducted at the site. Notably, Atekwana et al. (2014) investigated magnetic susceptibility variability in boreholes at the site in order to identify zones where microbial-mediated iron reduction is occurring. Atekwana et al. (2014) observed that magnetic susceptibility values were highest within the smear zone, which were also coincident with large concentrations of organic carbon and dissolved Fe(II) content, suggesting that the most biological activity occurs within the smear zone. Lund et al. (2017) also investigated the magnetic susceptibility using down hole MS logging data in boreholes in Bemidji. The study focused on a multi-year analyses of MS along with redox conditions and iron availability to assess whether MS can serve as a proxy in HC contamination monitoring. Coinciding with solid phase iron

depletion in the source zone, the MS response also diminished during the sampling period. The study confirmed MS response gives evidence for changing conditions of iron cycling and stability of iron minerals, however MS does not provide a proxy for long-term hydrocarbon biodegradation monitoring. In another study, Mewafy et al. (2013) performed laboratory studies on samples taken from the spill site focusing on frequency domain induced polarization and magnetic susceptibility. Knowing the site is characterized by a biogeochemical process where iron reduction is coupled with the oxidation of hydrocarbon contaminants, the main objective of their study was to elucidate the major factors controlling the complex conductivity response at the site. Results showed the magnitude of the real and imaginary components of the complex conductivity was higher for most of the samples from the smear zone compared to the dissolved phase saturated zone. The saturated zones of enhanced complex conductivity responses were concomitant with zones of high concentration of dissolved Fe (II) and enhanced magnetic susceptibility. This suggests that the complex conductivity response is driven by the presence of bio-metallic iron mineral phases such as magnetite resulting from the microbial oxidation of the coupling between hydrocarbons and iron reduction. Ultimately, Mewafy et al. (2013), suggested that the presence of metallic biominerals, such as magnetite, enhances the responses of complex conductivity in hydrocarbon contaminated areas exhibiting iron reduction as the dominant bio-physicochemical process.

CHAPTER III

METHODOLOGY

Overview of Surface Wave Method

We used the Multichannel Analysis of Surface Wave (MASW) method, proposed by Xia et al. (1999), to estimate shear wave velocity (V_S) from Rayleigh wave data. Provided is a brief summary of the method, and we point the reader to the original reference for details. The MASW method incorporates both active and passive sources. Xia et al. (1999) assumed that ground roll made up the most dominant signal in a seismic gather. Ground roll, which is mainly composed of surface waves, are both guided and dispersive. MASW is a seismic method, which generates a shear-wave velocity (V_S) profile (i.e. V_S versus depth) by analyzing Rayleigh-type surface waves on a multi-channel record. MASW utilizes the energy that is commonly considered noise on conventional seismic surveys. The fundamental mode of ground roll (the Rayleigh-type surface wave event) is the greatest source-generated noise on reflection surveys. It is noted that during the dispersion of surface waves, different frequencies (wavelengths) have different speeds (phase velocity), and the function of V_S changes with depth. The MASW technique is the best seismic technique for measuring the modulus of base materials and subgrade material. The entire procedure for MASW usually consists of

three steps: 1) acquiring multichannel records (or shot gathers), 2) extracting the fundamental-mode dispersion curves (one curve from each record), and 3) inverting these curves to obtain 1-D depth V_S profiles which are interpolated to result in a two-dimensional V_S image.

The phase velocity of a Rayleigh-wave is the function of a combination of parameters including S-wave velocity (V_S), P-wave velocity (V_P), layer thickness, and density (ρ). S-wave velocities however, have the most dominant effects on a dispersion curve when the frequencies are greater than 5 Hz (*Xia et al., 1999*). Through a detailed analysis of the Jacobian (J) matrix through a modeling aspect (Equations 1 and 2) and from borehole S-wave velocity measurements, S-wave velocity dominance is confirmed while noting that the phase velocity sensitivity to S-wave velocity is depth dependent (*Xia et al., 1999*).

$$\boldsymbol{J} = \left[\frac{\delta F/\delta V_{si}}{\delta F/\delta C_R}\right] \quad \textbf{(1)}$$

Where F is a nonlinear function of frequency, C_R is phase velocity, and V_{si} is S-wave velocity.

$$\boldsymbol{J\Delta m = \Delta d} \quad \textbf{(2)}$$

In which **m** is the model vector representing V_S, and **d** is the data error vector representing C_R.

Field Acquisition

Two parallel seismic profiles were acquired across the contaminated site (Figure 3) both stretching from the NW to SE roughly 25 meters apart. Transect 1 is represented by the blue dotted line, while transect 2 runs directly parallel to the former railroad line, and is shown by the red dotted line. Both transects started and ended outside of the plume, while covering the entire plume extent.

Each profile was acquired using 48 receivers with a geophone spacing of 2 meters and a shot spacing of 4 meters. The geophones used were vertical component with resonance frequency of 10 Hz. The MASW method incorporates both active and passive sources, however, we only used an active source in our data acquisition. The sources used were point explosives created by using a Betsy Seisgun and 400-grain 8-gauge blank shells. No filters were applied in the field, and a total of 24 shot records for Transect 1 and 25 for Transect 2 were used. The sample interval of the field data was 0.125 ms and the trace length was 1s.

Surface Wave Inversion

Both of our profiles were acquired using a static array, meaning every shot was recorded by every receiver (Fig. 6a). Using the SurfSeis software package developed by the Kansas Geological Survey (KGS), each trace was regrouped to ensure the dispersion curves were comparable from one location to another, while a fixed number of traces were cut and appended for each individual shot, instead of assuming that every receiver records every shot. In doing so, this established the correct roll-along type of acquisition needed from the static before. Similarly to Sharma (2017), the maximum offset for the

roll-along geometry was established by using a trial-and-error type method, so that the fundamental mode dispersion issued high energy pertaining to all records used for analysis and to improve lateral resolution. In doing this, a receiver spread of 6 geophones showed optimal results (Fig. 6b and 6c). Each shot gather was transformed to frequency-phase-velocity (f-V) domain (Fig. 6d) in order to estimate a specific dispersion curve (*Park et al., 1998)*. A 1D V_S profile (Fig. 6e) was then estimated from the dispersion curve of each shot gather using an iterative inversion algorithm, which uses a least-squares approach that allows for automation of the inversion process (*Xia et al., 1999).* An initial model consisting of a combination of several parameters was developed before searching for the optimum solution. These parameters include V_S, P-Wave velocity (V_P), Poisson's ratio (σ), density (ρ), and thickness (h). The initial V_S layer model is approximated from the measured dispersion curve (*Ismail et al., 2014).*An assumed constant ρ of 2.0 g/cc is assigned to all layers of the initial model, while the V_P model is determined using the V_S model and an assumed constant σ of 0.45. Using an iterative manner while converging toward the optimum solution, the initial model consists of 10 layers. Only V_S is updated after each iteration due to Rayleigh waves being most sensitive to V_S, while all other parameters are kept constant. The initial model V_S and depth of penetration (Z_f) are values are selected by making the assumption that V_S at a depth Z_f is 1.09 times the measured phase velocity (*Park et al., 1999).* Since equal numbers of gathers could be collected from either direction along each survey line, the final V_s models only show results pertaining to common gathers. Throughout the data set, parts of the data was aliased as shown in figure 7, however most of the frequency range (below 55 Hz) was not aliased and sufficient for processing. Although initial spread

lengths of each transect were collected at an approximate length of 192 meters, after data was cut, bad data points were omitted, and common data points were used, each profile length was approximately 96 meters in length.

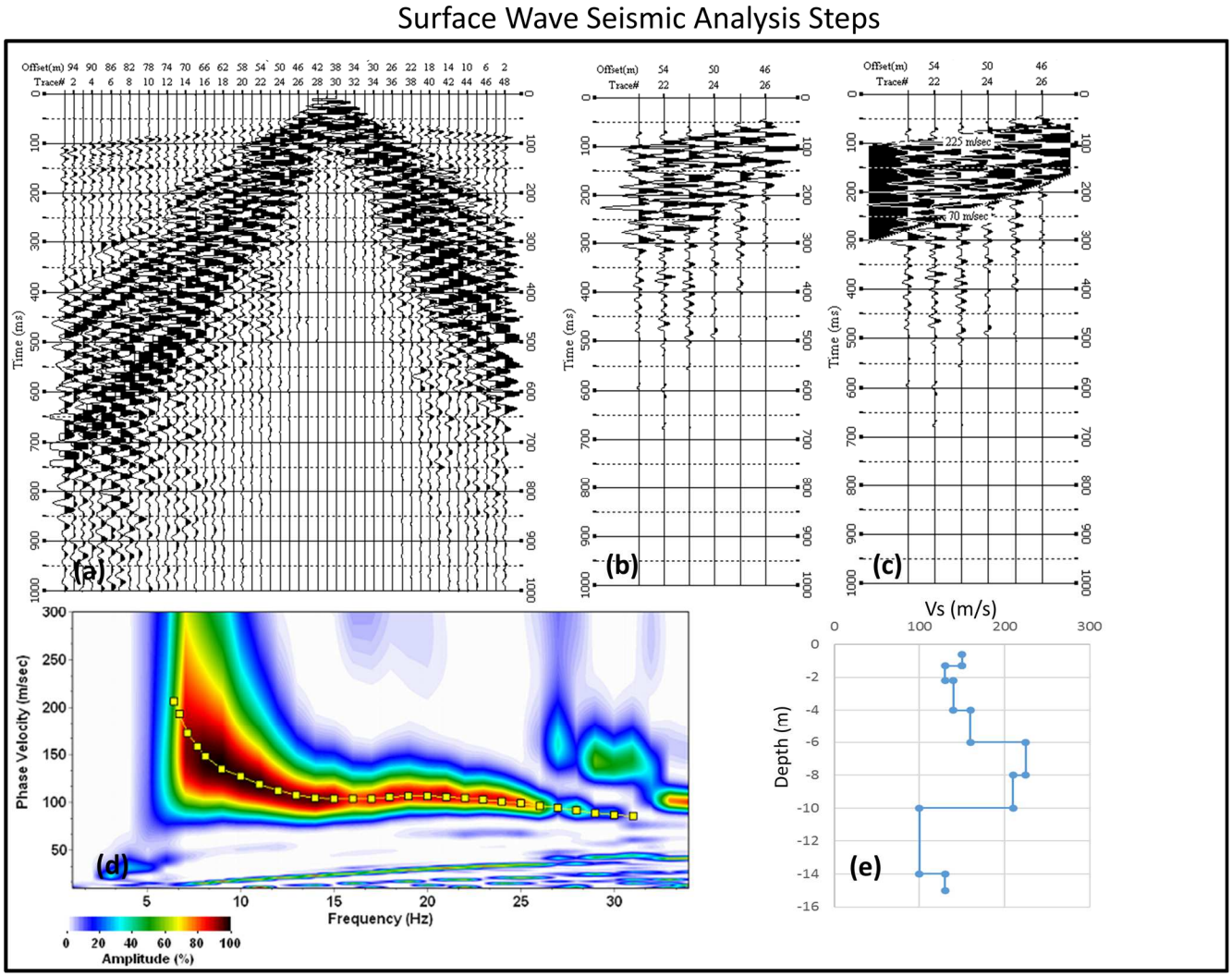

Figure 6 - Example of a surface wave seismic record and the output of the analysis steps, a) 48-trace raw record, b) extracted 12-trace record for the surface wave analysis to improve the lateral resolution, c) the 12-trace record with the velocity ranges displayed, d) the dispersion curve from the 12-trace record, and e) the velocity inversion of the dispersion curve.

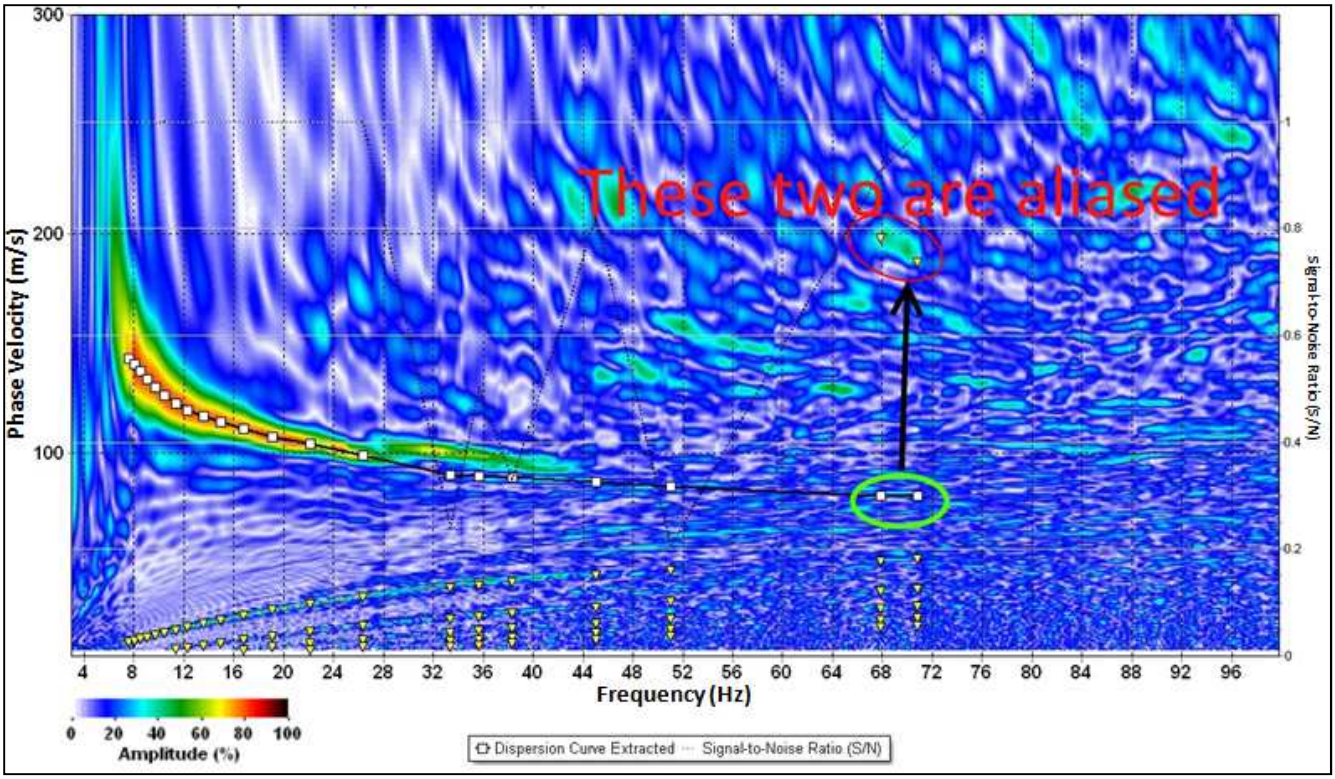

Figure 7 – Dispersion curve display over one shot record showing aliased frequencies, which are labeled in red. All data under 55Hz was not aliased and sufficient for processing. Image credit; Julian Ivanov, KGS.

Core Retrieval and Methods

Figure 3 above shows a map and locations of cores retrieved and used for magnetic susceptibility and core analysis since 2011. Six total cores were taken and analyzed between the years 2016 and 2017. Sediment cores were retrieved in a core barrel containing polycarbonate liners pushed into the sediment ahead of a hollow stem auger using the "freezing drive shoe" technology developed by USGS scientists. The freezing drive shoe enables nearly complete core recovery from saturated, sandy aquifers.

Cores were then sealed, frozen, and transported to Oklahoma State University (Stillwater, OK) for further analysis. Of these six cores, core descriptions were performed on cores 1604, 1709, and 1713 due to their close proximity to the seismic transects and were all located within the floating crude oil portion of the plume. Core descriptions were performed in the Biogeophysics Laboratory at Oklahoma State University. The three cores were sampled every 1/3 meter and analyzed by color content, sediment size, thickness, and composition.

CHAPTER IV

RESULTS

Seismic Transects

Two dimensional (2D) V_S models were interpolated from the individual 1D profiles as shown in figure 6.

Transect 1

Figure 8 represents the seismic section from transect 1. Three distinct shear wave velocity layers are observed. We observed a top layer from 0-4 meters depth, showing a velocity range from ~50-110 m/s, an intermediate layer from 5-7 meters depth, with a velocity range of ~150-250 m/s, and a lower, or bottom layer, from 8-14 meters depth with a velocity ranging between ~50 and 110 m/s. Assuming that the background shear wave velocity is around ~50-110 m/s, it appears that the middle layer has a V_S increase of greater than 80%. The average water table fluctuation zone within the past 15 years has been superimposed on the V_S model, along with dashed red lines, showing the approximate extent of the plume. As shown, the average water table depth on transect 1 is around six meters with a fluctuation of one meter. The increased shear wave velocity along the profile extends across the entire transect, and is not limited to the extent of the

plume. Also noted is the slight rise in depth along with higher velocities within the location of the hydrocarbon contaminated plume and the varying attenuation within the high velocity layer as well. It appears that the high velocity layer stays fairly consistent with the water table fluctuation zone, although is slightly lower on each end of transect 1, outside of the plume boundary, and has a slightly higher velocity as well.

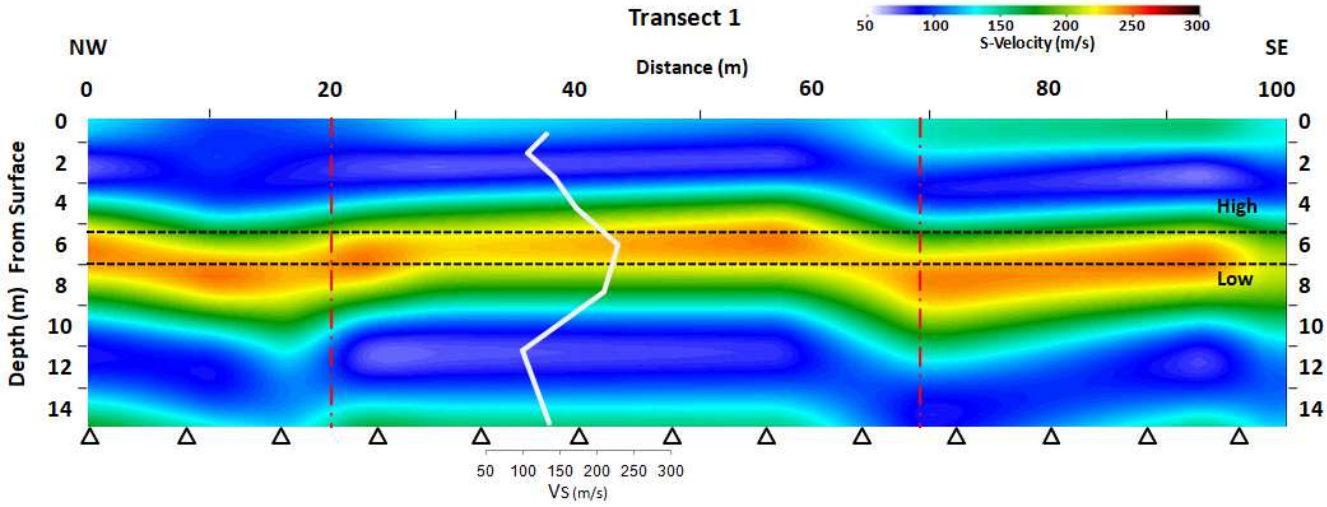

Figure 8 - Vs solution from Rayleigh wave inversion for Transect 1. Individual 1D Vs profiles were generated every 8m (shown by triangles) and interpolated to create this 2D image, example shown at 40m. Dashed red lines approximate extent of the plume. Dotted black lines represent the historic water table fluctuation along the transect measured from water observation wells and are labeled. Noted is the increase in S-velocity around the average water table fluctuation zone.

Transect 2

Figure 9 shows the seismic model of transect 2, which shows three distinct velocity layers. The upper layer ranges from 0-5 m and has a velocity between ~75-100 m/s, the middle layer ranges from 7-10 m with a velocity between ~210-250 m/s, and the

bottom layer ranges from 12-15 m exhibiting a velocity between ~80-125 m/s. Assuming the background velocity is around ~80-125 m/s, transect two also shows a large increase in shear wave velocity of greater than ~70-80%.

A 15 year average water table fluctuation level is plotted on Figure 9, along with the approximate extent of the plume. The average water table for transect 2 is around 8 m with a fluctuation of 1 m. Similar to transect 1, the high velocity layer extends along the entire transect and is not limited to just the plume extent, and also has some attenuation of velocity within the plume itself. It appears that the high velocity layer stays fairly consistent with the water table fluctuation zone, although a larger increase in velocity on the outside of the plume in each direction is noted as well. Noted is the high velocity layer slightly beneath the water table fluctuation zone to the SE end of the profile as well.

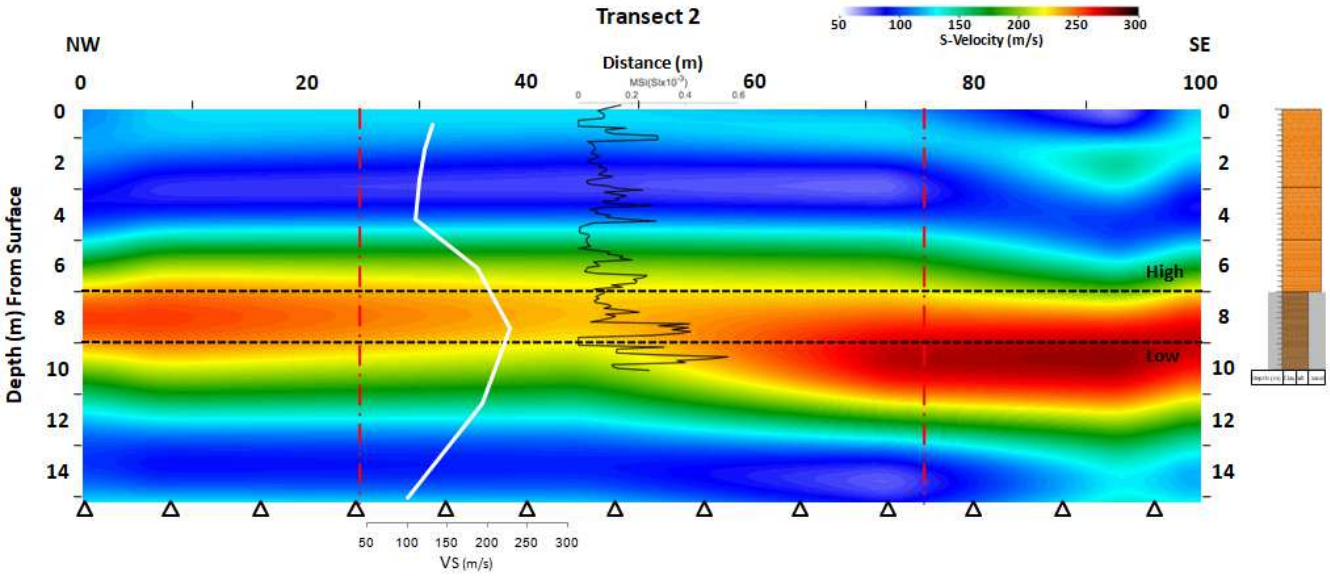

Figure 9 - Vs solution from Rayleigh wave inversion for Transect 2. Individual 1D Vs profiles were generated every 8m (shown by triangles) and interpolated to create this 2D image, example shown at 32m. Dashed red lines approximate extent of the plume. Dotted

black lines represent the historic water table fluctuation along the transect measured from water observation wells and are labeled. Stratigraphic column on far right created from core 1604 description; shaded layer indicates zone of hydrocarbon saturation, further explained below. Towards the center of the transect, magnetic susceptibility data for core 1407 is overlain. Noted is the increase in S-velocity and general increase/spike in MS response around the average water table fluctuation zone.

Core Description

Core 1604

The sediments from 0-3 m were light brown, medium fine sand with few to no pebbles. From 3-5 m the sediments were fine to very fine sand of light brown color with more noticeable pebble sized grains, followed by a 2 meter interval of similar color consisting completely of very fine grained sand to clay up to 7 meters down. Finally from 7 meters until the end of the core at approximately 10 meters, a gradual transition from brown, very silty clay to darker colored, oil stained, coarse grained sand with larger pebbles was identified at the end of the core.

Core 1709

This core showed medium brown colored, fine grained sand from 0-2 meters. From 2 to 3 meters the same colored sand was noticeable with fine to medium sized sand

grains turning into a lighter color of brown/tan towards the bottom. A small piece of the core was missing just after 3 meters, but from 3.75-6.75 meters, a light brown fine sized sand stretched the entire section. From 6.75 meters up to 8 meters the light brown sand turned into a very fine clay-like sediment. From 8 meters to the end of the core at 10 meters, the fine clay-like sediment turned a darker color brown to black and was oil saturated.

Core 1713

The final core, 1713, was similar throughout the first 3 m, consisting of a medium brown color, fine sandy sediment with few small pebbles. From 3 to 6 m, a medium brown colored, fine grained silt to sand was found throughout. At approximately 6 m until the end of the core at 9 m depth, a mostly fine silt layer characterized the zone with a litter darker brown to black color and was completely oil saturated.

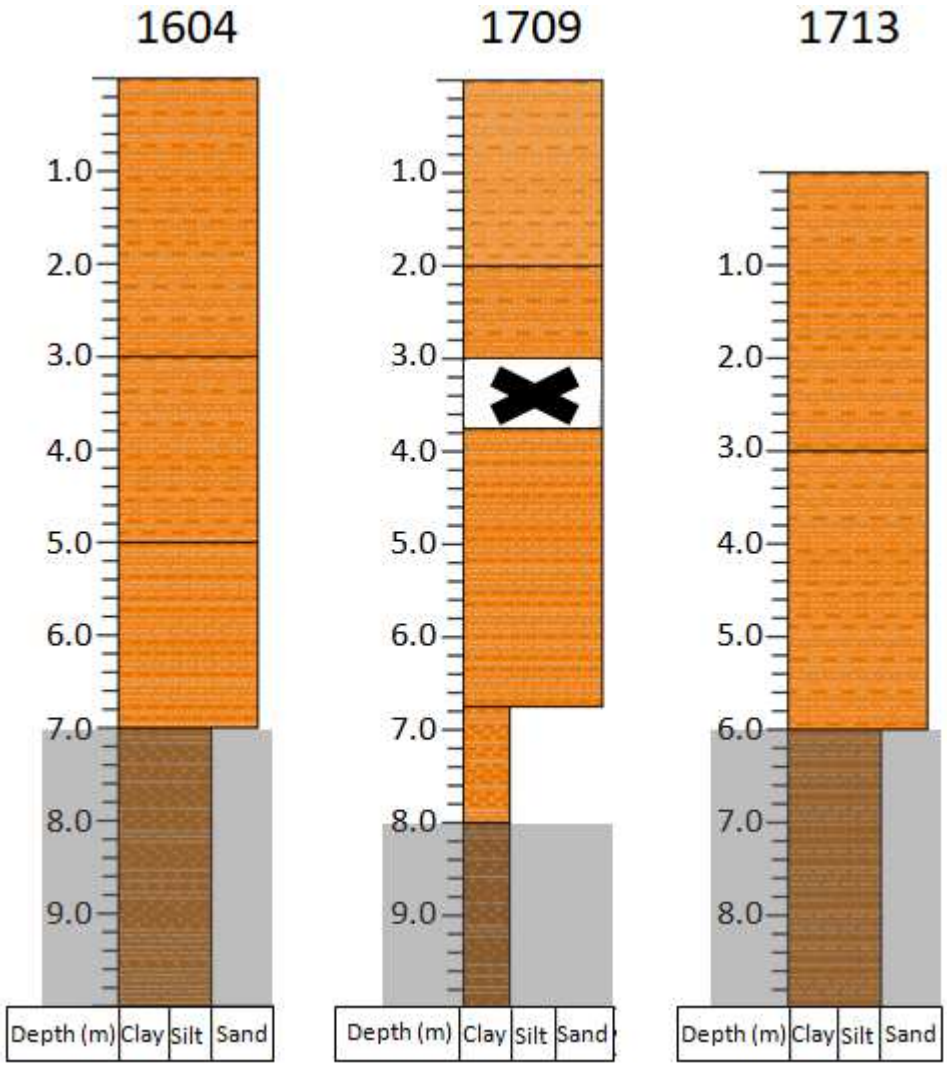

Figure 10 – Stratigraphic sections of each core created from individual core descriptions. Shaded layer indicates zone of hydrocarbon saturation. Black X on core 1709 indicates missing core.

Averaging the water table values within the past 15 years, and accounting for the approximate 1 meter of fluctuation that occurs along these transects, we focus in on the core descriptions between 5 and 9 meters. Shown in Figure 10 above, within this zone on

all three cores, a fine grain sandy silt to clay composition characterizes this zone, but no abrupt changes in lithology occur directly above or beneath. In each core, a darker, oil staining occurs at approximately 6-8 meters, likely representing the smear zone (absorption of free hydrocarbons floating on the water table onto aquifer solids), which is enhanced by the water table fluctuation zone. The smear zone is dominated by free and residual hydrocarbon contamination with variable thickness of up to 2 m (*Essaid et al., 2011)*.

CHAPTER V

DISCUSSION

Variability of Shear Waves as a Function of Depth

On transect 1, the increased velocity between 5-7 m bgs occurs within the fluctuating water table (Fig. 8). The upward displacement zone of higher velocity within the plume extent, between 20 to 70 m may be of significance. However, we suggest this could be a possible artifact of processing. Results of Transect 2 are similar to Transect 1, with the high velocity layer also occurring within the zone of water-table fluctuation. However, we also note an apparent decrease in the V_S within the plume boundaries. The findings within each seismic transect is the noticeable relationship between the increased velocity layer and the water table fluctuation zone. In each case, whether the water table is shallow (around 6 meters in transect 1) or deeper (around 8 meters in transect 2), the anomalous S-wave zone essentially occurs at the water-table fluctuation depth. The first question that arises is whether the coincidence between the water table fluctuation zone and S-wave anomalous zone is related to changes in lithology or rather, rheology.

To determine if the changes in S-Wave are due to variations in lithology, we refer to the geological cross section in Figure 4, as well as the core descriptions. Ismail et al.

(2014) conducted a study of seismic characterization of glacial sediments in central Illinois, similar to the geology found in our study site. They were able to suggest a V_S ranging from 85 to 700 m/s within these unconsolidated glacial sediments, confirming our velocities shown in the 2D profiles plausible. The Bemidji geological cross section (Fig. 4) shows no major changes in lithology across the water table. The sediments within the water table fluctuation zone and where the S-wave is higher are described as a laminated silt, very fine sand, and clay unit roughly 6 m bgs and extending up to 20 m in thickness. The sediments from the cores along each transect (from 5-9 m) are a fine grain sand to silt, with no abrupt lithologic changes directly above or below the water table fluctuation zone (Fig. 10). Based on the geologic cross section, core descriptions and the basic principle that the water table is independent of lithological variations in unconsolidated material, it is likely that the S-wave velocity changes across the water table are not due to lithologic changes.

Effect of Biogeochemical Processes on Shear Wave Velocity

Since the S-wave velocity anomaly is not a result of lithologic changes within the water-table fluctuation zone, we hypothesize that biogeochemical processes occurring within the water table could affect the shear modulus. Geochemical studies at the Bemidji site suggest that iron reduction and methanogenesis are the main terminal electron acceptor processes occurring at the site (*Baedecker et al., 1993*). In the study by Atekwana et al (2014), higher magnetic susceptibility measurements were found within the free product plume compared to the dissolved plume, suggesting that under optimum conditions, high organic carbon content, a fluctuating water table zone, and fluctuating redox conditions, microbial activity is accelerated. On Figure 9, magnetic susceptibility

from core 1407 (Figure 3), located near transect 2, has been overlain on the 2D profile. The most dominant area of increased MS values occurs within the water table fluctuation zone, similar to results found by Atekwana et al. (2014), likely indicating the precipitation of magnetite resulting from the biological activity stimulated in the water table fluctuation zone.

Changes in the Rheology of the Water Table Fluctuation Zone

The velocity of a shear wave is controlled by the shear modulus. Shear wave velocity is equivalent to the square root of the shear modulus divided by the solid's density. As shear waves propagate through the subsurface, the subsequent velocity will change based on the stiffness or rigidity of the material. The idea that increased biogeochemical activity can cause this increase in shear modulus and hence velocity increase, can be postulated in two ways: by the precipitation of minerals or by biofilms. The accumulation of biofilms, or potentially precipitation of minerals, has the ability to cause increases in contact areas between and amongst grains, resulting in increases in shear wave propagation (*Sharma, 2017)*. Precipitation of minerals such as magnetite, siderite, and calcite can increase the stiffness of materials resulting in a velocity increase. For example, Dejong et al. (2006) was able to detect a rate of change in observed V_S during maximum cementation, resulting from microbial induced calcite precipitation in a lab setting. Ng et al. (2014) inferred a large siderite precipitation rate occurring at the Bemidji site, which could affect the rigidity of the materials causing a possible increase in velocity. However, Atekwana et al. (2014) suggested that magnetite was the dominant solid mineral phase within the zone of peak magnetic susceptibility at Bemidji. Accordingly, the plume would have higher biological activity. Results of the Atekwana et

al. (2014) study showed high MS values within plume regions, but did not show significant magnetite precipitation outside of the plume. With the high S-wave velocity layer extending from non-plume areas into plume areas, we know magnetite precipitation cannot indicate this response.

Ruling out magnetite precipitation as a possible cause of the velocity increase, the next possible cause could be biofilms. Noh et al. (2016), building on previous studies that focused on compressional wave signatures, conducted a laboratory experiment that investigated shear wave velocity response to biofilm. Over a 38 day biostimulated column experiment, they noted minimal changes occurring in P-wave velocity, but increases of greater than 50% in S-wave velocity due to biofilm growth. This study, together with the Sharma (2017) field study, both point to biofilms as a possible cause of S-wave velocity increase. With our knowledge of the fact that biological activity is driven by the water table fluctuation, which occurs both inside and outside the plume, the accumulation of biofilms is a plausible explanation for our S-wave velocity increase. The Sharma (2017) study confirmed biofilm accumulation using Environmental Scanning Electron Microscope (ESEM) imaging within the water table fluctuation zone, however their study profile was only located within the plume, and it is unclear to determine what results would have looked like outside of the plume. To confirm biofilm evidence within our study area, ESEM images are shown below from core 1407 (contaminated region) and core 1408 (uncontaminated region) taken from within the WTFZ (Figure 11).

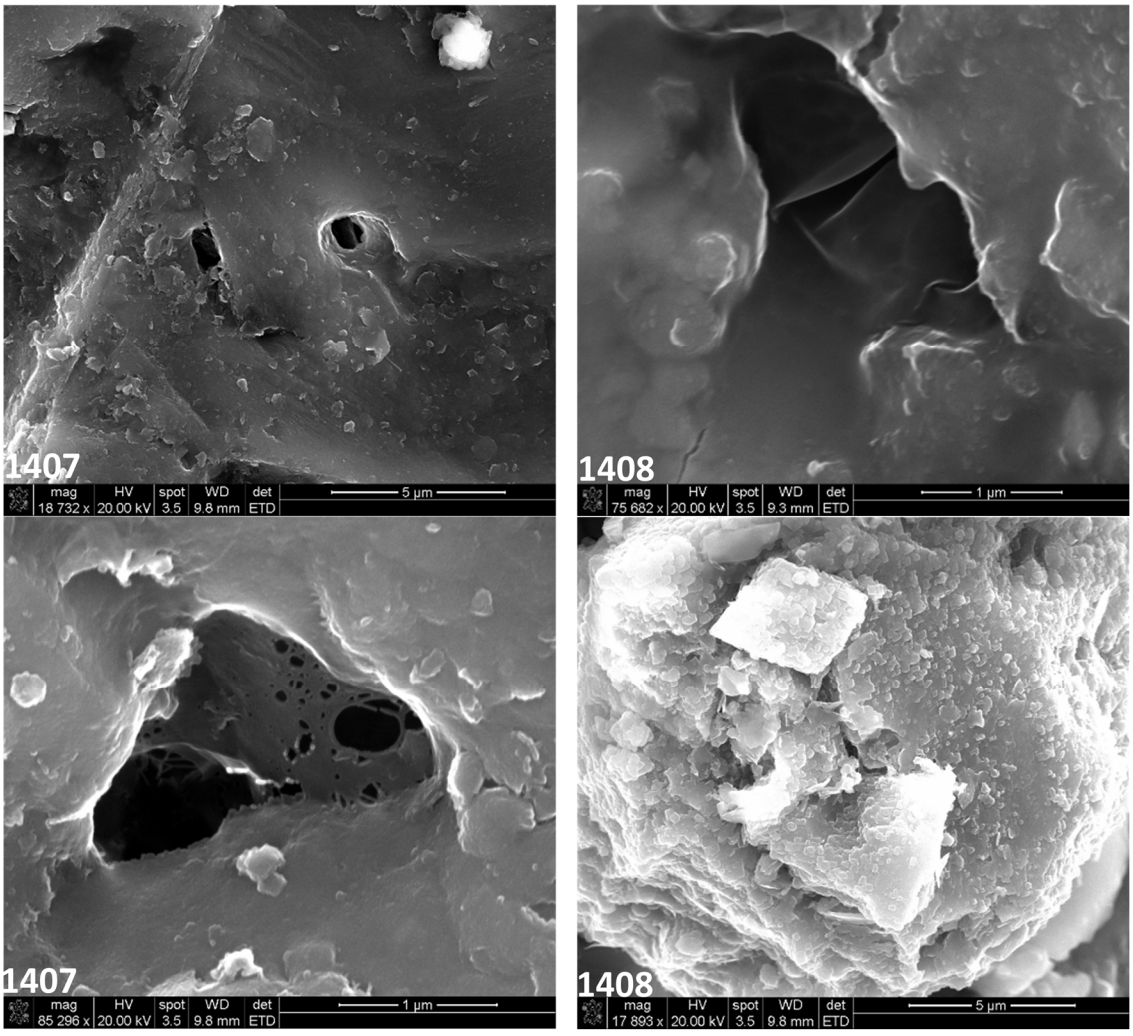

Figure 11 – Environmental Scanning Electron Microscope images confirming biofilm growth both within the water table fluctuation zone. Images on the left are from core 1407 located inside the plume, while images on the right are from core 1408 located outside the plume. Images courtesy of Dr. Estella Atekwana.

As can be seen on Figure 11, ESEM images from within the plume as well as outside the plume boundaries confirm the presence of biofilms. The confirmation of biofilms outside of the plume may offer an explanation to the increased velocity layer extending beyond the plume extent, though further analysis should be completed.

V_S Changes Within the Hydrocarbon Contaminant Plume and Beyond the Contaminant Plume

Understanding the influence that transient redox conditions, caused by the water table fluctuations and how they enhance microbial oxidation, as Rezanezhad et al (2014) explained, makes it easier to explain the results depicted by our transect profiles. Knowing that the water table alone cannot have an effect on shear wave seismic or the shear modulus, it is postulated that the changes occurring within the water table fluctuation zone, unique to each transect, are caused by the increased biogeochemical processes occurring at the site. McClain et al (2003) hypothesized that microbial activity is stimulated in biogeochemical transition zones, which is consistent with the findings that microbial community biomass was clearly elevated at the redox transition (*Stegen et al., 2016)*.

S-Wave velocities ranging from around 220-240 m/s within the plume, to greater than 250 m/s outside of the plume, could be indicative of areas of increased geochemical activity, and signify hot spots. In each profile, a slight attenuation of S-Wave velocity within the intermediate layer is observed inside the plume boundaries. This slight decrease in velocity inside the plume could be related to gas production occurring within the plume and not outside (*Priest et al., 2006)*. Another observation, occurring between 80 and 100 meters on transect 2 is a slight velocity draw down of the high velocity layer, likely caused by the layer/artifact located at 2 meters directly above. We postulate that the increased biogeochemical activity, nutrient supply, and microbially activity, increases biofilm production, which in turn increases the shear modulus recorded. Higher shear wave velocity increases may be linked to biogeochemical hot spots, and can be used to

predict better sampling areas for further research. The extension of the increased shear wave velocities outside the plume are a product of hydrologic processes occurring spatially, and would be beneficial to study more in depth. Extending the work of Sharma (2017), we believe that our study has shown that seismic is able to record the end product of biogeochemical processes driven by hydrologic processes and potentially can help predict hot spot locations cheaper and minimally invasively for future research work.

CHAPTER VI

CONCLUSIONS

In extending the study of Sharma (2017), we investigated the ability of using minimally invasive surface seismic techniques to detect the end product of biogeochemical processes driven by hydrologic processes. The main goals in the study were to verify that shear wave velocities are enhanced within the water table fluctuation zone due to enhanced microbial activity, and to determine if any differences in shear wave velocities between contaminated and uncontaminated regions of the study site existed. Generating V_S from ground roll using the MASW method, we observed a large increase in S-wave velocity within the water table fluctuation zone on two separate seismic transects, each with a different water table depth. Subtle differences in velocities were analyzed between contaminated and uncontaminated regions, although the highest velocities occurred outside the plume. We confirm that the fluctuating water table effects the biogeochemistry which in turn drove the geophysical changes. For increased confidence and results, recommendation of acquiring multiple, better quality seismic transects would be beneficial. Extending the transects both vertically and horizontally across the plume extent, with a smaller spacing between geophones could potentially give

beneficial results. In addition to multiple seismic transects ran, more current magnetic susceptibility measurements, along with scanning electron microscopy (SEM) imaging of multiple cores both within and outside the plume would be encouraged to better understand the biogeochemical processes occurring and biofilm evidence. However, with the knowledge learned from this study, it is easy to see that surface seismic techniques could be used in conjunction with other geophysical methods, for possibly imaging and identifying these biogeochemical hot zones in the subsurface and helping guide microbial and geochemical sampling so that these zones can be better studied and understood.

REFERENCES

Ahmed Ismail, Andrew Stumpf and Robert Bauer, 2014: Seismic characterization of glacial sediments in central Illinois. Journal of Applied Geophysics, Volume 101, p.1–10. http://dx.doi.org/10.1016/j.jappgeo.2013.11.009

Ahmed Ismail, F. Brett Denny, Mohamed Metwaly, 2014: Comparing continuous profiles from MASW and shear-wave reflection seismic methods. Journal of Applied Geophysics, Volume 101, p.67–77

Atekwana, E. A., and L. D. Slater (2009), Biogeophysics: A new frontier in Earth science research, Rev. Geophys., 47, RG4004, doi:10.1029/2009RG000285.

Atekwana E., Atekwana E.. Geophysical signatures of microbial activity at hydrocarbon contaminated sites: a review, *Surv. Geophys.* , 2010, vol. 31 2(pg. 247-283)

Atekwana, E., Mewafy, F., 2014. High-resolution magnetic susceptibility measurements for investigating magnetic mineral formation during microbial mediated iron reduction. J. Geophys. Res. Biogeosciences 1–15. doi:10.1002/2013JG002414.Received

Baedecker, M. J., I. M. Cozzarelli, J. R. Evans, and P. P. Hearn (1992), Authigenic mineral formation in aquifers rich in organic material, in *Proceedings of the 7th International Symposium on Water□Rock Interaction*, edited by Y. K. Kharaka and A. S. Maest, pp. 257–261, A. A. Balkema, Rotterdam.

Baedecker, M. J., I. M. Cozzarelli, R. P. Eganhouse, D. I. Siegel, and P. C. Bennett (1993), Crude□oil in a shallow sand and gravel aquifer: 3. Biogeochemical reactions and mass□balance modeling in anoxic groundwater, *Appl. Geochem.*, **8**(6), 569–586.

Beaver, C. L., Williams, A. E., Atekwana, E. A., Mewafy, F. M., Abdel Aal, G., Slater, L. D., & Rossbach, S. (2016). Microbial Communities Associated with Zones of Elevated Magnetic Susceptibility in Hydrocarbon-Contaminated Sediments. *Geomicrobiology Journal*, 1-12. DOI: 10.1080/01490451.2015.1049676

Bennett, P. C., D. E. Siegel, M. J. Baedecker, and M. F. Hult (1993), Crude-oil in a shallow sand and gravel aquifer 1. Hydrogeology and inorganic geochemistry, Appl. Geochem., **8**(6), 529–549.

Blodau, C., Moore, T.R., 2003. Micro-scale CO2 and CH4 dynamics in a peat soil during a water fluctuation and sulfate pulse. Soil Biol. Biochem. 35, 535–547.

Bekins, B. A., I. M. Cozzarelli, E. M. Godsy, E. Warren, H. I. Essaid, and M. E. Tuccillo (2001), Progression of natural attenuation processes at a crude oil spill site: II. Controls on spatial distribution of microbial populations, *J. Contam. Hydrol.*, **53**(3–4), 387–406.

Cozzarelli, I. M., B. A. Bekins, M. J. Baedecker, G. R. Aiken, R. P. Eganhouse, and M. E. Tuccillo (2001), Progression of natural attenuation processes at a crude-oil spill site: 1. Geochemical evolution of the plume, J. Contam. Hydrol., **53**(3–4), 369–385.

Craig, L., Bahr, J. M. & Roden, E. E. Localized zones of denitrification in a floodplain aquifer in southern Wisconsin, USA. Hydrogeol. J. 18, 1867–1879 (2010)

Davis, C. A., L. J. Pyrak-Nolte, E. A. Atekwana, D. D. Werkema, and M. E. Haugen, 2009, Microbial-induced heterogeneity in the acoustic properties of porous media: Geophysical Research Letters, 36, L21405, doi: 10 .1029/2009GL039569.

Davis, C. A., Pyrak-Nolte, L.J., Atekwana, E. a., Werkema, D.D., Haugen, M.E., 2010. Acoustic and electrical property changes due to microbial growth and biofilm formation in porous media. J. Geophys. Res. 115, 1–14. doi:10.1029/2009JG001143

DeJong, J. T., B. M. Mortensen, B. C. Martinez, and D. C. Nelson (2010), Bio□mediated soil improvement, Ecol. Eng., 36, doi:10.1016/j.ecoleng. 2008.12.029.

Delin, G. N., H. I. Essaid, I. M. Cozzarelli, M. H. Lahvis, and B.

A.Bekins (1998), Ground water contamination by crude oil near Bemidji, Minnesota, *U.S. Geological Survey Fact Sheet FS*, 84–98.

Drenovsky, R.E., Vo, D., Graham, K.J., Scow, K.M., 2004. Soil water content and

organic carbon availability are major determinants of soil microbial community composition. Microb. Ecol. 48, 424–430.

Eganhouse, R. P., M. J. Baedecker, I. M. Cozzarelli, G. R. Aiken, K. A. Thorn, and T. F.

Dorsey (1993), Crude oil in a shallow sand and gravel aquifer: II, Org. Geochem., Appl. Geochem., **8**, 551–567.

Essaid, H. I., B. A. Bekins, W. N. Herkelrath, and G. N. Delin (2011), Crude oil at the

Bemidji site: 25 years of monitoring, modeling, and understanding, Ground Water, **49**(5), 706–726.

Griffiths, B.S., Hallett, P.D., Kuan, H.L., Pitkin, Y., Aitken, M.N., 2005. Biological and

physical resilience of soil amended with heavy metal-contaminated sewage sludge. Eur. J. Soil Sci. 56, 197–206.

Haberer, C.M., Rolle, M., Cirpka, O.A., Grathwohl, P., 2012. Oxygen transfer in a

fluctuating capillary fringe. Vadose Zone J. 11 (3). http://dx.doi.org/10.2136/ vzj2011.0056.

Hancock, P.J., Boulton, A.J., Humphreys, W.F., 2005. Aquifers and hyporheic zones:

towards an ecological understanding of groundwater. Hydrogeol. J. 13, 98–111.

Hedin, L. O. et al. Thermodynamic constraints on nitrogen transformations and other

biogeochemical processes at soil-stream interfaces. Ecology 79, 684–703 (1998).

Heenan, J., L. D. Slater, D. Ntarlagiannis, E. A. Atekwana, B. Z. Fathepure, S. Dalvi, C.

Ross, D. D. Werkema, and E. A. Atekwana, 2015, Electrical resistivity imaging for long-term autonomous monitoring of hydrocarbon degradation: Lessons from the Deepwater Horizon oil spill: Geophysics, 80, no. 1, B1-B11.

Hefting, M., Clément, J.C., Dowrick, D., Cosandey, A.C., Bernal, S., Cimpian, C., Tatur,

A., Burt, T.P., Pinay, G., 2004. Water table elevation controls on soil nitrogen cycling in riparian wetlands along a European climatic gradient. Biogeochemistry 67, 113–134.

Hult, M.F. 1984. Ground-water contamination by crude oil at the Bemidji, Minnesota, research site – An introduction. In Ground-water Contamination by Crude Oil at the Bemidji, Minnesota, Research Site–U.S. Geological Survey Toxic Waste–Ground-Water Contamination Study Papers Presented at the Toxic-Waste Technical Meeting, ed. M.F. Hult. Tucson, Arizona, March 20– 22. U.S. Geological Survey Water-Resources Investigations Report 84-4188, Chap. A, 1–15.

Kwon, T., Ajo-franklin, J.B., 2013. High-frequency seismic response during permeability reduction due to biopolymer clogging in unconsolidated porous media. Geophysics 78, EN117-EN127. doi:doi:10.1190/geo2012-0392.1

Lovley, D. R., M. J. Baedecker, D. J. Lonergan, I. M. Cozzarelli, E. J. P. Phillips, and D.

Siegel (1989), Oxidation of aromatic contaminants coupled to microbial iron reduction, *Nature*, **339**(6222), 297–300.

Lund, A.L., Slater, L.D., Atekwana, E.A., Ntarlagiannis, D., Cozzarelli, I., and Bekins,

B.A., 2017, Evidence of coupled carbon and iron cycling at a hydrocarbon-contaminated site from time lapse magnetic susceptibility: Environmental Science and Technology, v. 51, no. 19, p. 11244-11249, doi:10.1021/acs.est.7b02155.

McClain, M. E. et al. Biogeochemical hot spots and hot moments at the interface of

terrestrial and aquatic ecosystems. Ecosystems 6, 301–312 (2003).

Mewafy, F. M., D. D. Werkema, E. A. Atekwana, L. D. Slater, G. Z. Abdel Aal, A.

Revil, and D. Ntarlagiannis (2013), Evidence that bio□metallic mineral precipitation enhances the complex conductivity response at a hydrocarbon contaminated site, *J. Appl. Geophys.*, **98**, 113–123.

Nevin, K. P., D. E. Holmes, T. L. Woodard, E. S. Hinlein, D. W. Ostendorf, and D. R.

Lovley (2005), Geobacter bemidjiensis sp. nov. and Geobacter psychrophilus sp. nov., two novel Fe(III)□reducing subsurface isolates, *Int. J. Syst. Evol. Microbiol.*, **55**(4), 1667–1674.

Ng GHC, Bekins BA, Cozzarelli IM, Baedecker MJ, Bennett PC, Amos RT. A mass

balance approach to investigating geochemical controls on secondary water quality impacts at a crude oil spill site near Bemidji, MN. Journal of Contaminant Hydrology. 2014;164(0):1–15.

Noh, D., Ajo-franklin, J.B., Kwon, T., Muhunthan, B., 2016. P and S wave responses of

bacterial biopolymer formation in unconsolidated porous media 1–20. doi:10.1002/2015JG003118.Received

Park, Choon Byong, Richard D. Miller, and Jianghai Xia (1998) Imaging dispersion curves of surface waves on multi□channel record. SEG Technical Program Expanded Abstracts 1998: pp. 1377-1380. https://doi.org/10.1190/1.1820161

Pett-Ridge, J., Firestone, M.K., 2005. Redox fluctuation structures microbial communities in a wet tropical soil. Appl. Environ. Microbiol. 71, 6998–7007.

Pett-Ridge, J., Silver, W.L., Firestone, M.K., 2006. Redox fluctuations frame microbial community impacts on N-cycling rates in a humid tropical forest soil. Biogeochemistry 81, 95–110.

Priest, J. A., A. I. Best, and C. R. I. Clayton (2006), Attenuation of seismic waves in methane gas hydrate-bearing sand, Geophys. J. Int., 164(1), 149-159.

Rezanezhad, F., R.□M. Couture, R. Kovac, D. O'Connell, and P. van Cappellen (2014), Water table fluctuations and soil biogeochemistry: An experimental approach using an automated soil column system, *J. Hydrol.*, 509, 245–256.

Rijal, M. L., E. Appel, E. Petrovsky, and U. Blaha (2010), Change of magnetic properties due to fluctuations of hydrocarbon contaminated groundwater in unconsolidated sediments, *Environ. Pollut.*, **158**(5), 1756–1762.

Schimel, J., Balser, T.C., Wallenstein, M., 2007. Microbial stresses response physiology and its implications for ecosystem function. Ecology 88, 1368–1394

Sharma, S., Atekwana, E., Jaiswal, P., Vilcaez, J. (2017), In-Situ Biofilm Detection Using Seismic Methods

Sophocleous, M., 2002. Interactions between groundwater and surface water: the state of the science. Hydrogeol. J. 10, 52–67.

Stegen JC, et al. Coupling among microbial communities, biogeochemistry, and mineralogy across biogeochemical facies. Sci. Rep. 2016;6:30553. doi: 10.1038/srep30553.

Stegen, J. C., Lin, X., Konopka, A. E. & Fredrickson, J. K. Stochastic and deterministic assembly processes in subsurface microbial communities. ISME J. 6, 1653–1664 (2012).

Triska, F.J., Kennedy, V.C., Avanzino, R.J., Zellweger, G.W., Bencala, K.E., 1989. Retention and transport of nutrients in a third-order stream in northwestern California: hyporheic processes. Ecology 70, 1893–1905.

Tuccillo, M. E., I. M. Cozzarelli, and J. S. Herman (1999), Iron reduction in the sediments of a hydrocarbon□contaminated aquifer, *Appl. Geochem.*, **14**(5), 655–667.

Vorenhout, M., van der Geest, H.G., van Marum, D., Wattel, K., Eijsackers, H.J.P., 2004. Automated and continuous redox potential measurements in soil. J. Environ. Qual. 33, 1562–1567.

Weber, F.-A., Voegelin, A., Kaegi, R., Kretzschmar, R., 2009. Biogenic copper(0) and metal sulphide colloids mobilize contaminants in flooded soil. Nat. Geosci. 2, 267–271.

Xia, J., Miller, R.D., Park, C.B., 1999. Estimation of near-surface shear-wave velocity by inversion of Rayleigh waves. Geophysics 64, 691. doi:10.1190/1.1444578

Zachara, J. M., R. K. Kukkadapu, P. L. Gassman, A. Dohnalkova, J. K. Fredrickson, and T. Anderson (2004), Biogeochemical transformation of Fe minerals in a petroleum□contaminated aquifer, *Geochim. Cosmochim. Acta*, **68**(8), 1791–1805.

VITA

Braden Hrencher

Candidate for the Degree of

Master of Science

Thesis: HYDROLOGIC PROCESSES AT INTERFACES CAUSE CHANGES IN GEOPHYSICAL SIGNATURES: A FIELD STUDY

Major Field: Geology

Biographical:

Education:

Completed the requirements for the Master of Science in your Geology at Oklahoma State University, Stillwater, Oklahoma in May, 2018.

Completed the requirements for the Bachelor of Science in your Geology at Fort Hays State University, Hays, Kansas in May, 2015

Experience:

- Geophysics Intern – Devon Energy, Oklahoma City, OK : Summer 2017
- Teaching and Research Assistant – Oklahoma State University, Stillwater, OK : August 2015 – May 2017

Professional Memberships:

- Society of Exploration Geophysicists
- Geological Society of America
- American Association of Petroleum Geologists